International Journal of Computer Science and Information Technology
ISSN: 3005-9682 (Print), ISSN: 3005-7140 (Online) | Volume 2, Number 3, Year 2024
DOI: https://doi.org/10.62051/ijcsit.v2n3.28
Journal homepage: https://wepub.org/index.php/IJCSIT/index

A Study of Multibeam Line Measurement Problems Based on Analytic Geometry and Mechanistic Analysis

Yucheng Liu, Qi Huang*, Junsong Liu

School of Mathematics and Science, Chengdu University of Technology, Yibin Campus, Yibin, China

*Corresponding Author: 1084217627@qq.com

ABSTRACT

Based on the important application of multibeam bathymetric systems in marine science and engineering, this study explores their working principle and application potential. Through the establishment of a mathematical model, problems such as coverage width and distance between survey lines are solved, and an optimized survey line layout scheme is proposed. For the seabed topography data, combined with geometric analysis and visualization technology, accurate measurement and analysis of seabed topography is realized, which provides important support for marine survey, resource exploration and underwater engineering. The research results are of guiding significance for the further development and application of multibeam bathymetry technology and provide strong support for research and practice in related fields.

KEYWORDS

Multibeam Sounding, Analytical Geometry, Mechanism Analysis

1. INTRODUCTION

Multibeam bathymetric systems (MBES), as an advanced marine survey technology, have demonstrated great potential and importance in the field of marine science and engineering [1]. By utilizing the ultrasonic principle, MBES can comprehensively measure bathymetric strips in flat areas of the seafloor and provide detailed data on seafloor topography, as well as identify potential obstacles and geomorphic features. The wide range of applications of such systems covers many fields such as marine surveying, resource exploration and underwater engineering, providing important support for marine scientific research and marine engineering construction [2].

The aim of this thesis is to explore the working principle and application potential of MBES and to solve the related problems by establishing mathematical models. Through the geometric relationship model and the knowledge of analytical geometry, we analyze the problems of coverage width, survey line layout optimization and shortest survey line length, which provide useful guidance for optimizing the practical application of multibeam bathymetric systems. In addition, we analyzed and processed the seafloor topography data in detail and explored the characteristics of seafloor topography and its role in system optimization. These research results will provide important references for the further development of multibeam bathymetry technology and marine scientific research and promote the development and application of this field.

Content from this work may be used under the terms of CC BY-NC 4.0 licence (https://creativecommons.org/licenses/by-nc/4.0/).
Published by Warwick Evans Publishing.

2. MULTIBEAM BATHYMETRIC COVERAGE WIDTH AND OVERLAP RATE MODELING

2.1. Definition of survey line overlap rate

According to the overlap rate when the survey lines are parallel to each other and the seafloor topography is flat to each other, we define the slope overlap rate [3]. The slope is shown schematically in Figure 1.

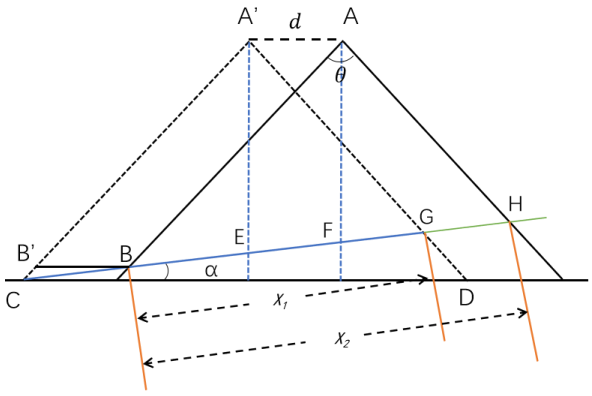

Figure 1. Schematic diagram of the slope

Point A is a measuring line point, A' is the previous measuring line point, C, B, E, F, G, H is the intersection of the slope and the beam. Where X_1 is the overlap width, X_2 is the coverage width, which defines the overlap rate between the current survey line and the previous survey line in Figure 1 as:

$$\eta = \frac{X_1}{X_2} \tag{1}$$

Make a parallel of AA' through point B to intersect $A'C$ at B', $BB' = AA' = d$, then we have $\angle A'CE = 30° - \alpha$,$\angle CB'B = 90° + \theta/2$,in $\triangle CB'B$ by the sine theorem:

$$CB = \frac{d \cdot \sin \angle CBB'}{\sin \angle CB'B} = \frac{d \cdot \sin\left(90° + \frac{\theta}{2}\right)}{\sin(30° - \alpha)} \tag{2}$$

Let x denote the distance from the current line of measurement to the center point, and let the coverage width at this line of measurement be W_i, and the coverage width of the previous line of measurement be W_{i-1}, then X_2 is denoted as W_i, at this place, then,

$$\eta = \frac{W_{i-1} - \frac{d \cdot \sin\left(90° + \frac{\theta}{2}\right)}{\sin\left(90° - \alpha - \frac{\theta}{2}\right)}}{W_i} \tag{3}$$

2.2. Geometric modeling of the central sea area

This sea area is essentially a plane geometry problem, so we create a plane image based on point A of this central sea area, as shown in Figure 2.

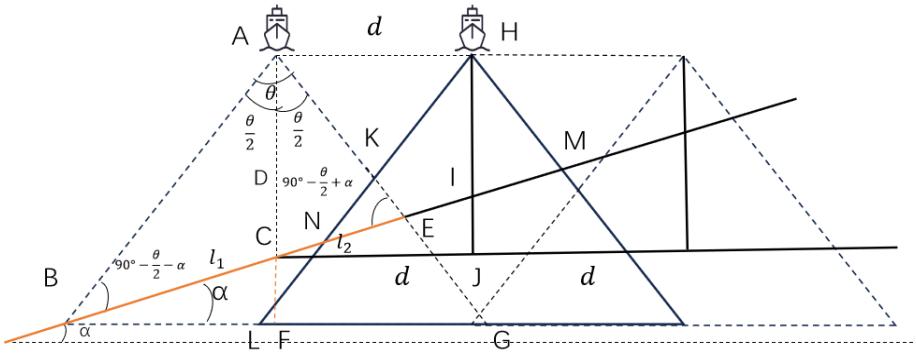

Figure 2. Geometric model of the center of the sea area

In Figure 2, the intersection points of the sea center point A and the seabed are B,E, and the intersection points of point H and the seabed are M,N. AC is the depth of seawater at the center point of the sea, and HI is the depth of seawater at point H. $BC = l_1$, $CE = l_2$, $AC = D$. The center point A is the depth of seawater at the center point of the sea.

In $\triangle ABC$, by the sine theorem we have,

$$\frac{l_1}{\sin\left(\frac{\theta}{2}\right)} = \frac{D}{\sin\left(90-\frac{\theta}{2}-\alpha\right)} \tag{4}$$

Similarly, in $\triangle ACE$,

$$\frac{l_2}{\sin\left(\frac{\theta}{2}\right)} = \frac{D}{\sin\left(90-\frac{\theta}{2}+\alpha\right)} \tag{5}$$

Coverage width,

$$W_1 = l_1 + l_2 \tag{6}$$

Analyze with the center of the sea area to the right, where $CJ = d$, set $IJ = X_1$,$HI = \mathrm{D}_1$,$NI = l_3$, $IM = l_4$. In $\triangle HNI$,

$$\frac{l_3}{\sin\left(\frac{\theta}{2}\right)} = \frac{D_1}{\sin\left(90-\frac{\theta}{2}+\alpha\right)} \tag{7}$$

In $\triangle HIM$,

$$\frac{l_4}{\sin\left(\frac{\theta}{2}\right)} = \frac{D_1}{\sin\left(90-\frac{\theta}{2}+\alpha\right)} \tag{8}$$

Coverage width,

$$W_2 = l_3 + l_4 \tag{9}$$

From (2) the overlap rate,

$$\eta = \frac{NE}{NM} \tag{10}$$

In $\triangle ICJ$,

$$\tan\alpha = \frac{X_1}{d} \tag{11}$$

Sea depth,

$$D_1 = D - X_1 \tag{12}$$

The model developed from the above analysis can be solved for the data values of seawater depth and coverage width.

2.3. Solving the model

The opening angle of the multibeam transducer is 120°, the slope is 1.5°, and the depth of seawater at the center point of the sea area is 70 m. Substitute the relevant data into the above model.

The specific values of the solved seawater depth and coverage width are shown in Table. 1.

Table 1. Determination of seawater depth and coverage width

Distance from center	Sea depth	Coverage width	Overlap rate
-800	90.95	315.81	-----
-600	85.71	297.63	32.80
-400	80.47	279.44	28.43
-200	75.24	261.26	23.45
0	70.00	243.07	17.72
200	64.76	224.88	11.07
400	59.53	206.70	3.24
600	54.29	188.51	-6.09
800	49.05	170.33	-17.42

3. THREE-DIMENSIONAL COVERAGE WIDTH AND OVERLAP RATE MODELING

3.1. Establishment of spatial coordinate system

First of all, we establish a three-dimensional spatial coordinate system, with the projection of the slope surface normal to the horizontal plane of the line where the x-axis, perpendicular to the direction of the horizontal plane is the z-axis, the y-axis that is perpendicular to the x-axis on the horizontal plane of the straight line where the specific parameters and identification as shown in Figure 3.

SC is the projection of the survey line on the horizontal plane, SB is the projection of the survey line on the slope surface, $\triangle SAD$ is the slope cross-section, and quadrilateral $ABCD$ is a rectangle. Because the sea area is a three-dimensional image, we need to transform the three-dimensional image into a two-dimensional image and find the slope value $\alpha'$of the two-dimensional image, which can be solved using the model in the previous section.

The process of solving for α' is as follows:

Set $AD = x,\ BC = AD = x$, then in $\triangle SAD$:

$$SD = x \cdot \tan\alpha \tag{13}$$

In $\triangle SDC$,$\angle DSC = 180° - \beta$,then there is:

$$SC = \frac{x \cdot \tan\alpha}{\cos(180° - \beta)} \tag{14}$$

So, in $\triangle SBC$.

$$\tan' = \frac{\cos(180° - \beta)}{\tan\alpha} \tag{15}$$

Then the two-dimensional slope,

$$\alpha' = arc\tan\frac{\cos(180° - \beta)}{\tan\alpha} \tag{16}$$

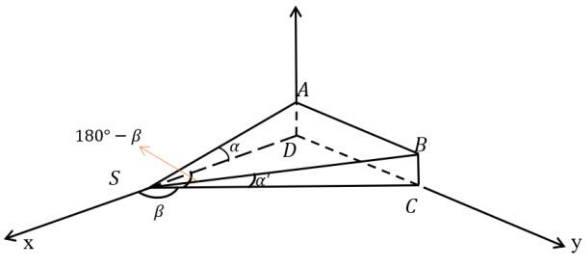

Figure 3. Three-dimensional map of the sea area

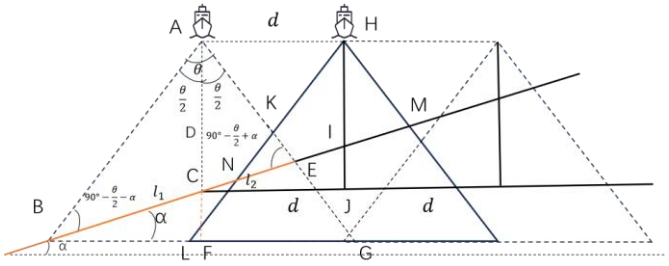

Figure. 4 Two-dimensional slope map

3.2. Solving the 2D slope surface

The transformed 2D image is shown in Figure 4.

Let point A be the starting point of the ship's survey line, the depth of seawater at this point is x, the coverage width is W,the coverage rate is η, and the spacing between neighboring survey points is d, where $d = 0.3$, then based on the model that has already been established in the previous section, it can be obtained,

$$\frac{l_4}{\sin\left(\frac{\theta}{2}\right)} = \frac{x}{\sin\left(90-\frac{\theta}{2}-\alpha'\right)} \tag{17}$$

$$\frac{l_5}{\sin\left(\frac{\theta}{2}\right)} = \frac{x}{\sin\left(90-\frac{\theta}{2}+\alpha'\right)} \tag{18}$$

$$W = l_4 + l_5 \tag{19}$$

$$\eta = \frac{NE}{NM} \tag{20}$$

Based on the above model, the values of the coverage width of the multibeam bathymetry with respect to the direction of the survey line and the distance of the survey vessel from the center sea area can be solved, as shown in Table. 2.

Table. 2. Determination of coverage width

Coverage width			Distance from the center						
		0	0.3	0.6	0.9	1.2	1.5	1.8	2.1
Direction angle	0	416.69	467.21	517.73	568.25	618.77	669.29	719.81	770.33
	45	416.19	451.87	487.55	523.23	558.91	594.59	630.27	665.95
	90	415.69	415.69	415.69	415.69	415.69	415.69	415.69	415.69
	135	416.19	380.51	344.83	309.15	273.47	237.79	202.11	166.43
	180	416.69	366.17	315.65	265.13	214.61	164.09	113.57	63.05
	225	416.19	380.51	344.83	309.15	273.47	237.79	202.11	166.43
	270	415.69	415.69	415.69	415.69	415.69	415.69	415.69	415.69
	315	416.19	451.87	487.55	523.23	558.91	594.59	630.27	665.95

4. LINE LENGTH MODELING

4.1. Establishment of the sea area line measurement model

The three-dimensional schematic of the rectangular sea area is shown in Figure 5.

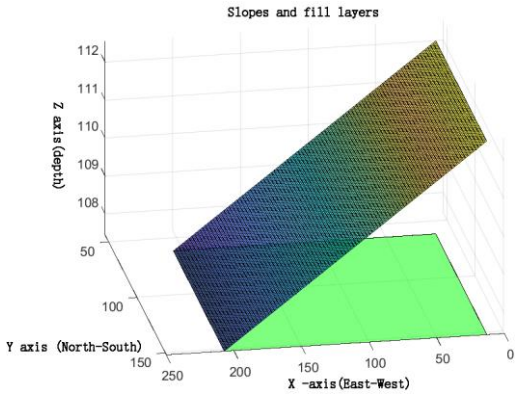

Figure 5. Three-dimensional diagram of the sea area

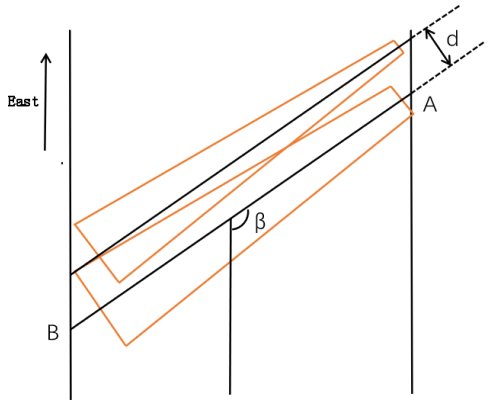

Figure 6. Top view of the sea area

The sea area is deep in the west and shallow in the east with a slope of 1.5°. Next, we analyze the sea area with a top view, as shown in Figure 6.

First, the survey lines in the region are parallel to each other due to the requirement of parallel distribution of ship survey lines. And, in order to satisfy that the entire rectangular sea area is covered, the maximum distance between survey lines is determined by the most under depth position on the seafloor through which the line passes, which we refer to simply as the short-plate effect.

We take the direction of the ship's survey line and the sea plane angle β to analyze, when β is 90 °, the length of the ship's survey line is the shortest. When β is greater than 90°, due to the influence of west depth and east shallowness and slope, point A moves eastward (upward in Figure 6), the narrower the width of the ship's survey line, and the wider the width of the ship's survey line when point A moves westward; when β is less than 90°, due to the influence of west depth and east shallowness and slope, the further eastward point B is (upward in Figure 6), the narrower the width of the ship's survey line, and the wider the width of the ship's survey line is when point B is further westward. And the larger the spacing d between boat survey lines, the shorter the total survey line length [4-5].

Now, we build the 2D plan view of the slope, as shown in Figure 7.

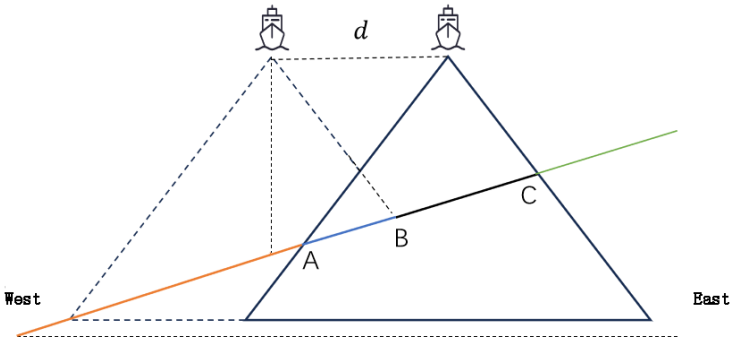

Figure. 7 Cross-section of the slope

Based on the above principle, in order to make the spacing d between the ship survey lines as large as possible, the AB spacing should be as small as possible, and when the AC length is fixed, due to the overlap rate formula (1), we conclude that the larger d is, the smaller the overlap rate is. Therefore, in order to meet the requirement of 10%-20% overlap rate, we control the overlap rate by 10%.

The overlap rate formula (2) is as follows:

$$\eta(x,d)=\frac{W_{i-1}-\frac{d\cdot\sin\left(90°+\frac{\theta}{2}\right)}{\sin\left(90°-\alpha-\frac{\theta}{2}\right)}}{W_i}=\frac{W_{i-1}}{W_i}-\frac{d\cdot\sin\left(90°+\frac{\theta}{2}\right)}{\sin\left(90°-\alpha-\frac{\theta}{2}\right)} \tag{21}$$

$$W_i=l_i+l_{i+1} \tag{22}$$

Where, x denotes the distance from the current survey line to the center point and denotes the interval of the previous survey line from the center point. Since the overlap rate is known to be 10% from above, d can be solved by calculation.

4.2. Data solving of the model

In summary, we have obtained a set of survey lines with the shortest measurement length and completely covering the whole sea area through MATLAB, where $\beta = 90°$.

The image of the specific sea measuring line is shown in Figure 8.

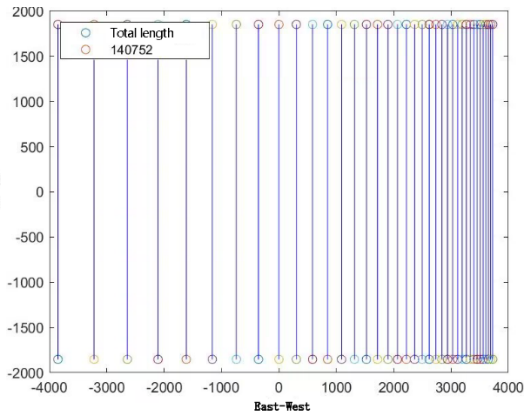

Figure 8. Sea area line survey map

The coordinates of the survey lines are shown in Table. 3 below:

Table. 3. Line coordinates

West-East coordinate	Route	West-East coordinate	Route	West-East coordinate	Route	West-East coordinate	Route	West-East coordinate	Route
0	-3851	6	-742	11	848	16	1899	21	2620
1	-3222	7	-356	12	1091	17	2066	22	2735
2	-2642	8	0	13	1316	18	2221	23	2841
3	-2108	9	304	14	1525	19	2364	24	2939
4	-1615	10	586	15	1719	20	2497	25	3030

5. MEASUREMENT WIRING MODEL

Firstly, we establish the seafloor topographic map based on the seafloor depth data, as shown in Figure 9.

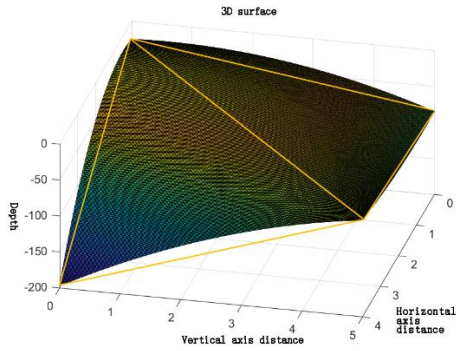

Figure 9. Topographic map of the seafloor

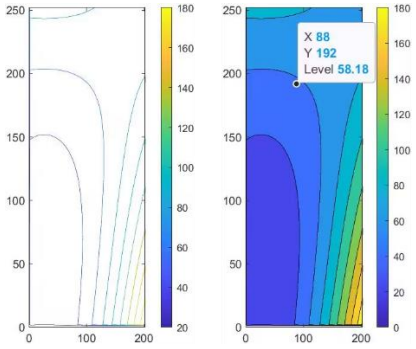

Figure 10. Variation of seafloor depth

We then use this to create a map of the depth variation of the seafloor, as shown in Figure 10.

From Figure 10, we can see that the seafloor topography is slightly higher on two sides and slightly lower on the other two sides. We connect the slightly higher points in Figure 9 and divide them into two triangular slopes.

We use Figure 9 as the basis and combine the data in Figure 10 to build the top view image, as shown in Figure 11.

We assume that $Z(x)$, where x denotes the depth of the seafloor at point Z, $A(84.4), B(65.2), C(24.4)$, and $D(197.2)$, and since $\triangle ABC$ is slightly higher than $\measuredangle BCD$, when we start the multibeam from $\measuredangle ABC$, if the line of measurement covers $\measuredangle ABC$, then the line of measurement will cover the whole $\triangle BCD$, and the overlap is larger because of the deeper depth of $\measuredangle BCD$. Because the depth of $\measuredangle BCD$ is deeper, the overlap rate is larger [6].

If we build a set of equipotential lines in $\measuredangle ABC$, it can be successfully transformed into the model in the previous section. Because the depth of the seabed at point A is 84.4, the depth of the seabed at point C is 24.4, and because the slope of the seabed is continuous, the straight line where AB is located must have a point with a height of 65.2, and this point is set as $E(65.2)$, as shown in Figure 12. A, E, C is located in a straight line vertically downward observation, to obtain the cross-section Figure 13.

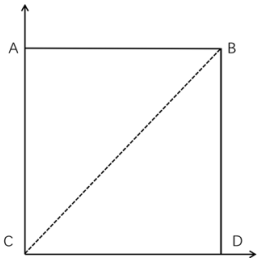

Figure 11. Overhead view of seafloor topography

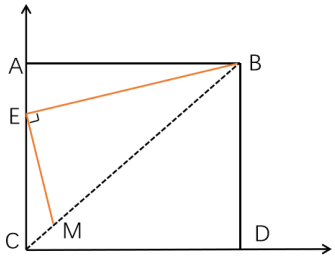

Figure 12. Top view

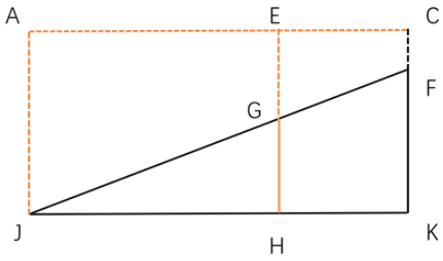

Figure 13. A, E, C cross section

The final values of the intersection of the measured line and the y-axis are shown in Table. 4.

Table. 4. Measured line and y-axis intersection values

Value of the intersection of the survey line with the y-axis										
5.0000	4.852	4.707	4.565	4.426	4.2899	4.1568	4.0265	3.8985	3.7735	3.6514
3.5316	3.414	3.299	3.1867	3.0768	2.9692	2.8634	2.7599	2.6587	2.5598	2.4627
2.3679	2.275	2.184	2.0946	2.0073	1.9218	1.8381	1.7561	1.6759	1.5973	1.5206
-1.2028	-1.220	-1.24	-1.2563	-1.2738	-1.2906	-1.3069	-1.3232	-1.3389	-1.3546	-1.3697
-1.3843	-1.400	-1.41	-1.4267	-1.4401	-1.4535	-1.4663	-1.4791	-1.4919	-1.5041	-1.5163
-1.5279	-1.540	-1.55	-1.5616	-1.5727	-1.5832	-1.5936	-1.6035			

We assume that the overlap rate of $\triangle ABC$ is floating around 10%, then the overlap rate of $\triangle BCD$ is greater than 10%, the known angle of inclination $\angle ABE$ = 21.60 °, and also know that the line of measurement and the angle of the Y-axis, it can be found that the total length of the line of measurement for the 571316.38 , and therefore the leakage of the sea area accounted for the percentage of the total area of the sea area to be measured is 0%.

6. CONCLUSIONS

As an advanced marine survey technology, multibeam bathymetric system (MBES) shows an important potential in the field of marine science and engineering. Through the mathematical model established in this paper, we deeply discuss the working principle and optimization method of MBES, which provides useful guidance for the practical application of the system. From the coverage width, survey line layout to the optimization of survey line length, we propose corresponding solutions, which provide theoretical support for the application of multibeam bathymetry. In addition, the detailed analysis and processing of seafloor topography data provide an important reference for system optimization, highlighting the influence of seafloor topography on system performance. By analyzing the seabed topography, we can better understand the working characteristics of the system and provide more accurate data support for marine scientific research and engineering construction.

To summarize, the prospect of the wide application of MBES in the marine field should not be neglected. This study lays a foundation for the further development and application of multibeam bathymetry technology, and at the same time provides strong support for marine scientific research and engineering practice and promotes the balanced development of marine resources development and environmental protection.

REFERENCES

[1] Šiljeg A, Marić I, Domazetović F, et al. Bathymetric Survey of the St. Anthony Channel (Croatia) Using Multibeam Echosounders (MBES)—A New Methodological Semi-Automatic Approach of Point Cloud Post-Processing[J]. Journal of marine science and engineering, 2022, 10(1): 101.

[2] Liu Y, Wu Z, Zhao D, et al. Construction of high-resolution bathymetric dataset for the Mariana Trench[J]. IEEE Access, 2019, 7: 142441-142450.

[3] Lucieer V, Picard K, Siwabessy J, et al. Seafloor mapping field manual for multibeam sonar[J]. Field Manuals for Marine Sampling to Monitor Australian Waters, eds R. Przeslawski and S. Foster (National Environmental Science Programme (NESP)), 2018: 42-64.

[4] Ferreira I O, Andrade L C, Teixeira V G, et al. State of art of bathymetric surveys[J]. Boletim de Ciências Geodésicas, 2022, 28: e2022002.

[5] Borrelli M, Smith T L, Mague S T. Vessel-based, shallow water mapping with a phase-measuring sidescan sonar[J]. Estuaries and Coasts, 2022, 45(4): 961-979.

[6] Lambertini A, Menghini M, Cimini J, et al. Underwater drone architecture for marine digital twin: Lessons learned from SUSHI DROP project[J]. Sensors, 2022, 22(3): 744.